

Multi-Lepton Probes of the Drell-Yan Production of Triplet Higgses

Siddharth P. Maharathy^{1,2,a}, Srimoy Bhattacharya^{1,b}, Andreas Crivellin^{3,4,c}, Mukesh Kumar^{1,d}, Rachid Mazini^{1,e}, and Bruce Mellado^{5,1,f}

¹ School of Physics and Institute for Collider Particle Physics, University of the Witwatersrand, Johannesburg, Wits 2050, South Africa

² Indian Institute of Science Education and Research Pune, Dr. Homi Bhabha Road, Pune 411008, India

³ Universitat Autònoma de Barcelona, 08193 Bellaterra, Barcelona

⁴ ICREA, Institució Catalana de Recerca i Estudis Avançats, Passeig de Lluís Companys 23, 08010 Barcelona, Spain

⁵ Institute of High Energy Physics, 19B, Yuquan Road, Shijing District, 100049, Beijing, China

Abstract. Excesses in di-photon, $Z\gamma$, and WW spectra indicate the existence of a new Higgs boson with mass 152 ± 1 GeV. However, no excess is observed in the ZZ channel. This pattern aligns with a Real Higgs Triplet model with hypercharge $Y = 0$ (Δ SM). A prediction of this model is the Drell-Yan production of scalars at the LHC, which dominantly decay to electroweak bosons, thus enhancing the cross sections of triboson channels such as WWZ , WZZ , and WWW . Interestingly, both ATLAS and CMS have reported higher-than-expected significances for such processes: 6.4σ (observed) vs 4.7σ (expected) in the VVZ (where $V = W$ or Z) channel and 4.4σ vs 3.6σ in WWZ , suggesting the possibility that these signals may be the manifestations of an extended Higgs sector. We investigate whether the Δ SM can account for these triboson excesses through electroweak production and decay of triplet scalars. We find that while current data prefers a non-zero new physics signal (2.6σ), the Δ SM predicts more events than observed, such that it is consistent with data but not preferred over the SM. However, this tension could be clarified with Run 3 and HL-LHC data.

1 Introduction

The 2012 discovery of the Higgs boson [1, 2] was a landmark achievement that completed the particle content of the Standard Model (SM). Despite its success, growing experimental anomalies suggest that the SM is not the complete description of nature [3]. The so-called “Multilepton anomalies” — statistically significant excesses observed in LHC data across several channels (see Refs. [3, 4] for recent reviews). These events feature multiple leptons (electrons and/or muons), moderate missing transverse energy, and (b) jets. The consistency of these anomalies across different final states points toward the presence of additional scalar resonances [5–8]. In particular, the mass of one of the scalars is predicted to be $m_S = 150 \pm 5$ GeV [6]. In this context, recent measurements have reported excesses

in di-photon [9, 10], $Z\gamma$ [11, 12], and WW [13–15] final states, providing strong indications in support of a new scalar particle with a mass 152 ± 1 GeV [16, 17]. Interestingly, no corresponding excess has been seen in the ZZ channel [18, 19], a pattern that poses a challenge for models involving a standard Higgs doublet or singlet extension. However, this pattern is naturally obtained if the new scalar is the neutral component of a hypercharge $Y = 0$ triplet [20, 21] and, in fact, the observed excesses can be partially explained by the Drell-Yan production of the triplet [22–25].

The Drell-Yan production of the neutral and charged components of the triplet can not only explain the excesses in associated di-photon production, but via its dominant decays to electroweak (EW) gauge bosons also leads to WWW , WWZ , and WZZ final states, which are currently under close experimental scrutiny. Intriguingly, both ATLAS and CMS have reported higher-than-expected significances for these processes. For example, 6.4σ vs 4.7σ in the VVZ channel [26] and 4.4σ vs (3.6σ) in WWZ [27]. Since the experimental searches are statistically uncorrelated, and the statistical uncertainties dominate over

^a e-mail: siddharth.prasad.maharathy@cern.ch

^b e-mail: srimoy.bhattacharya@cern.ch

^c e-mail: andreas.crivellin@cern.ch

^d e-mail: mukesh.kumar@cern.ch

^e e-mail: rachid.mazini@cern.ch

^f e-mail: bmellado@mail.cern.ch

the systematic ones, any correlations among them are expected to be small. The “multi-lepton anomalies” suggest the existence of a new scalar with a mass range of 150 ± 5 GeV that decays dominantly to W bosons and is produced in association with lepton, bottom quarks, and missing energy. Both the production and decay modes are in agreement with the triplet hypothesis. Importantly, these indirect hints for a new scalar reduce the look-elsewhere effect. In this analysis, we have not considered the CMS WWW analysis, since the CMS analysis requires a large $\Delta\phi$ cut requiring events with higher WWW invariant mass, which is not sensitive to NP at lower masses. This is illustrated in Table 1 and Fig. 1 where the measured signal strengths for these processes w.r.t. their values expected in the SM are shown.

So far, it has been shown that the SM supplemented with a $Y = 0$ triplet, the ΔSM is not excluded from multi-lepton searches [24, 28]. In this paper, we investigate whether the ΔSM , can accommodate the elevated multi-boson cross sections. We focus on the parameter space where the neutral component has a mass 152 ± 1 GeV, as suggested by the di-photon and $Z\gamma$ measurements, and the charged component must be quasi mass degenerate because of EW precision constraints. Using detailed Monte Carlo simulations, we analyse the production and decay of these triplet scalars and compute the predicted cross-sections for WWZ , WZZ , WWW and tWZ final states. We compare these predictions with the latest LHC measurements to assess the viability of the ΔSM in this context.

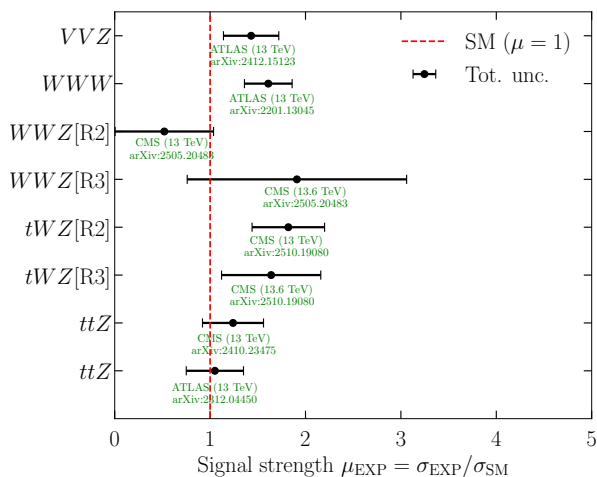


Fig. 1: Measured signal strengths relative to the expected SM values ($\mu_{\text{EXP}} = \sigma_{\text{EXP}}/\sigma_{\text{SM}}$) for each analysis along with their uncertainties. The total uncertainty is obtained by adding the statistical, systematic and the theory error in quadrature. R2 and R3 stand for Run 2 and Run 3, respectively. It is interesting to note that except for the Run 2 CMS analysis of WWZ , all values are above 1.

2 Signal regions and validation

In this article, we study analyses targeting three EW gauge bosons, $V = W, Z$, produced directly or indirectly via top decays done in the SM context. In Table 1, we summarise the ATLAS and CMS results for the different analyses that we consider in this work. Furthermore, the measured signal strengths normalised to their SM predictions (μ_{EXP}) for each process is illustrated in Fig 1.¹

To validate the setup for our analysis, we first simulated the SM processes for the different analyses using `MadGraph5_aMC_v3.5.3` [33, 34] for event generation. The obtained parton-level events are passed through the regular chain of tools, namely `Pythia 8.3` [35] and `Delphes 3.5.0` [36] (we will thus abbreviate our simulation with MPD), to obtain the result of subsequent decays of the unstable particles, radiations, showering, fragmentation, hadronisation as well as various detector effects and particle-level object reconstruction. We then implemented the respective cuts for each analysis. We explain each of the considered analyses in detail below.

The cutflows for the different signal regions for each considered analysis are shown in the appendix in Tables 3–11.

2.1 ATLAS (VVZ)

The ATLAS VVZ analysis consists of three signal regions (SRs) [26] containing three (3ℓ), four (4ℓ) and five (5ℓ) charged leptons ($\ell = e, \mu$) in the final state. These leptons are required to have a rapidity of $|\eta| < 2.47$ for electrons and $|\eta| < 2.7$ for muons. The transverse-momentum threshold for the leptons in the 3ℓ SR are $p_T > 27$ GeV, 15 GeV, and 15 GeV. Similarly, for the 4ℓ SR, ATLAS requires 4-leading leptons with $p_T > 30$ GeV, 15 GeV, 8 GeV, and 6 GeV. A Z -boson candidate is identified from a same-flavor opposite-sign lepton pair with an invariant mass requirement of $|m_{\ell\ell} - m_Z| < 20$ GeV, where $m_{\ell\ell}$ is the reconstructed same-flavor opposite-sign di-lepton invariant mass. Jets are reconstructed using the anti- k_T algorithm with radius parameter $R = 0.4$, requiring $p_T^j > 20$ GeV and $|\eta_j| < 5.0$. The overlap removal of leptons and jets is implemented according to the description of Ref. [26]. For the 3ℓ SR, in addition to the three leptons, at least one light jet is required, while b -tagged jets are vetoed in all three SRs.

To validate our setup, we simulated the SM processes $pp \rightarrow VVZ$, where $V = W, Z$. The number of expected events from the ATLAS simulation and our MPD one for the 3ℓ , 4ℓ and 5ℓ signal regions for an integrated luminosity

¹ For the ttZ signal strength, we used the digitized data of Refs. [31, 32].

CoM Energy	Process	Measured Cross Section [fb]	SM Cross Section [fb]	$\mu_{\text{EXP}} = \sigma_{\text{EXP}}/\sigma_{\text{SM}}$
$\sqrt{s} = 13$ TeV	VVZ [ATLAS]	$660^{+93}_{-90}(\text{stat.})^{+88}_{-81}(\text{syst.})$ [26]	461 ± 23 [26]	1.43 ± 0.29
	WWW [ATLAS]	$820 \pm 100(\text{stat.}) \pm 80(\text{syst.})$ [29]	511.0 ± 18 [29]	1.61 ± 0.25
	WWZ [CMS]	$97^{+91}_{-75}(\text{stat.})^{+24}_{-21}(\text{syst.})$ [27]	184 ± 9.2 [27]	0.52 ± 0.52
	tWZ [CMS]	$248 \pm 38(\text{stat.}) \pm 35(\text{syst.})$ [30]	136.0^{+9}_{-8} [30]	1.82 ± 0.38
	ttZ [CMS]	1224.6 ± 156.7 [31]	989 ± 49 [31]	1.24 ± 0.32
	ttZ [ATLAS]	$860 \pm 40(\text{stat.}) \pm 40(\text{syst.})$ [32]	860^{+80}_{-90} [32]	1.05 ± 0.30
$\sqrt{s} = 13.6$ TeV	WWZ [CMS]	$380^{+220}_{-190}(\text{stat.})^{+50}_{-30}(\text{syst.})$ [27]	200 ± 10 [27]	1.91 ± 1.15
	tWZ [CMS]	$242 \pm 62(\text{stat.}) \pm 46(\text{syst.})$ [30]	147.8^{+10}_{-9} [30]	1.64 ± 0.52

Table 1: Observed and expected SM values for the inclusive cross sections of VVZ , WWW , tWZ and ttZ production at the LHC. The total uncertainty of μ_{EXP} is obtained by adding all errors in quadrature.

of 139 fb^{-1} and 13 TeV center of mass (CoM) are

VVZ SM	3ℓ	4ℓ	5ℓ
ATLAS [26]	376	72	4
MPD	366	55	3

Summing the events in all signal regions, we find

$$\frac{N_{\text{SM}}^{\text{ATLAS}}}{N_{\text{SM}}^{\text{MPD}}} \approx 1.07. \quad (2)$$

The proximity to unity of this correction factor shows good agreement of our fast simulation with the full detector simulation of ATLAS. Since our analysis relies on the overall signal strength from the ATLAS VVZ measurement (see Table 1), and the individual signal strengths for each signal region are not provided, summing over all signal regions offers a reasonable approximation for comparison with our simulation.

2.2 ATLAS (WWW)

The signal regions considered in this analysis require events with exactly two and three leptons [29]. Electrons (muons) are required to satisfy $p_T > 20 \text{ GeV}$ and $|\eta| < 2.47$ ($|\eta| < 2.5$) excluding electrons within $1.37 < |\eta| < 1.52$. Jets are reconstructed using the anti- k_T algorithm with $R = 0.4$, requiring $p_T^j > 30 \text{ GeV}$ in the forward direction ($2.5 < |\eta_j| < 4.5$) and $p_T^j > 20 \text{ GeV}$ in the central region ($|\eta| < 2.5$). For the 2ℓ SR events are required to have exactly two same-charged leptons and at least two central jets with no b -tagged jets. The transverse-momentum of the leading lepton and the dilepton invariant mass should have $p_T > 27 \text{ GeV}$ and $40 \text{ GeV} < m_{\ell\ell} < 400 \text{ GeV}$. The required condition on the dijet invariant mass and the pseudorapidity separation between the two jets is $m_{jj} < 160 \text{ GeV}$ and $|\Delta\eta_{jj}| < 1.5$. Depending on the flavor of the two leptons, the 2ℓ SR is further sub-categorized into: ee -mode,

$e\mu$ -mode, and $\mu\mu$ -mode. The 3ℓ SR events are selected requiring exactly three leptons with the leading lepton having $p_T > 27 \text{ GeV}$, no b -tagged jets, and no same-flavor opposite-sign (SFOS) lepton pair.

For the SM WWW simulation, we follow the same procedure as we followed for the SM VVZ process i.e, the montecarlo events $pp \rightarrow WWW$ was generated by Madgraph, hadronization is performed by Pythia and detector response is considered by Delphes. The total number of events in the signal regions for the WWW process from the ATLAS analysis and our simulation compared to ATLAS is

WWW SM	2ℓ	3ℓ
ATLAS [29]	234	35
MPD	230	38

which shows a good agreement

$$\frac{N_{\text{SM}}^{\text{ATLAS}}}{N_{\text{SM}}^{\text{MPD}}} \approx 1.004. \quad (4)$$

To conclude this section, it is important to note that the corresponding results reported by the CMS experiment in Ref. [37] are not included in this study. This is motivated by the presence of selection requirements, such as those on the momentum of the three-lepton system and on the azimuthal angle between this system and the missing transverse momentum, which suppress the efficiency for the new physics scenarios considered here.

2.3 CMS (WWZ)

The CMS cross-section measurements of WWZ [27] production was done at $\sqrt{s} = 13 \text{ TeV}$ and 13.6 TeV , corresponding to a total integrated luminosity of 200 fb^{-1} . The main physics objects used in the analysis are leptons (e and μ), escaping particles (p_T^{miss}), and jets. The final states contain two W bosons and a Z boson decaying to

four isolated leptons, either directly or via intermediate tau decays. The leading (sub-leading) lepton in the event is required to have $p_T > 25(15)$ GeV, and the p_T of the third and fourth lepton is required to have $p_T > 10$ GeV. Muons and electrons are required to have $|\eta| < 2.4$ and 2.5 , respectively. Two of the four leptons are demanded to be consistent with originating from the decay of an on-shell Z boson: These two leptons, referred to as “ Z candidate leptons”, are required to be of the same flavor, to have opposite charges, and to form an invariant mass within 10 GeV of the known Z boson mass. The remaining two leptons must have opposite charges, and are referred to as “ W candidate leptons”. Depending upon the flavours of the W candidate leptons, events are further categorized as “opposite flavor” (OF: $e\mu$) or “same flavor” (SF: ee or $\mu\mu$). In the SF channel, the W candidate leptons are required to form an invariant mass more than 10 GeV away from the known mass of the Z boson; additionally, the m_{T2} variable [38, 39] (which is constructed from the transverse momenta of the W candidate leptons and the p_T^{miss}) must be greater than 25 GeV. Following the event selection requirement, the simulated SM

WWZ SM	Run 2 [138 fb $^{-1}$]	Run 3 [62 fb $^{-1}$]
CMS [OF]	7.29	3.63
CMS [SF]	4.38	2.2
MPD [OF]	6.1	2.4
MPD [SF]	3.4	1.3

For Run 2 and Run 3 simulations we have considered $\sqrt{s} = 13$ TeV and 13.6 TeV with integrated luminosities 138 fb $^{-1}$ and 62 fb $^{-1}$, respectively. The ratios for the number of events from the full detector simulations of ATLAS vs our fast simulation are

$$\frac{N_{\text{SM}}^{\text{ATLAS}}}{N_{\text{SM}}^{\text{MPD}}} \approx 1.4 \text{ (R2)}$$

$$\frac{N_{\text{SM}}^{\text{ATLAS}}}{N_{\text{SM}}^{\text{MPD}}} \approx 1.6 \text{ (R3)}$$

Taking into account that here 4 leptons are required, which makes the analysis very sensitive to efficiency and acceptance effects, the agreement is reasonable.

2.4 CMS (tWZ)

The CMS analysis [30] provides the first observation of single top quark production in association with a W and a Z boson. The data used for this analysis corresponds to center-of-mass energies of 13 TeV and 13.6 TeV with a total integrated luminosity of 200 fb $^{-1}$. The leptons ($\ell = e, \mu$) are required to have transverse momentum $p_T > 10$ GeV for events collected at $\sqrt{s} = 13$ TeV, and

$p_T > 15$ GeV for events collected at $\sqrt{s} = 13.6$ TeV. Jets are reconstructed using the anti- k_T algorithm with $R = 0.4$, requiring $p_T^j > 25$ GeV and $|\eta_j| < 2.5$. Events with at least three reconstructed leptons are constructed and the p_T of the leading lepton must have $p_T > 25$ GeV and the subleading one $p_T > 15$ GeV. An opposite-sign, same-flavor (OSSF) lepton pair is identified as a Z if its invariant mass $|m_{\ell\ell} - m_Z| < 15$ GeV. The signal region (SR) is divided into two parts, depending on the number of leptons: events with three leptons enter the SR $_{3\ell}$, while events with four leptons are assigned to the SR $_{4\ell}$. The SR $_{3\ell}$ signal region also requires at least two jets with one of them to be b -tagged, whereas the SR $_{4\ell}$ requires at least one b -tagged jet.

tWZ SM	Run 2 + Run 3 [200 fb $^{-1}$]
CMS	134
MPD	70

For Run 2 and Run 3 simulations we have considered $\sqrt{s} = 13$ TeV and 13.6 TeV with integrated luminosities 138 fb $^{-1}$ and 62 fb $^{-1}$, respectively. The ratios for the number of events from the full detector simulations of CMS vs our fast simulation are

$$\frac{N_{\text{SM}}^{\text{CMS}}}{N_{\text{SM}}^{\text{MPD}}} \approx 1.9 \text{ (R2 + R3)}$$

which is reasonable because of the high multiplicity final state with of 3ℓ and 4ℓ and additional (b)-jets. Note that in the NP analysis, we will always consider the ratio of the NP signal strength over that of our SM simulation, such that detector effects drop out to a good approximation

2.5 $t\bar{t}Z$

Here we reuse the results of our previous work, Ref [41], where we recasted $t\bar{t}Z$ analyses of ATLAS [32] and CMS [31] to search for signs of charged Higgs bosons and set novel limits on the product of branching fractions $\text{Br}(t \rightarrow \Delta^\pm b) \times \text{Br}(\Delta^\pm \rightarrow WZ)$. In Fig 4, we showed the NP Feynman diagram contributing to the SM $t\bar{t}Z$ process.

The CMS analysis provides differential cross sections for the sum of $t\bar{t}Z$ and tWZ production (within the SM), unfolded to the parton level (after radiation but before hadronization), as functions of 5 observable. The ATLAS analysis, on the other hand, reports $t\bar{t}Z$ differential cross sections unfolded to both particle and parton levels covering 15 observables. For the detailed information about the CMS and ATLAS observable, see [31, 32, 41]. The NP signal process $pp \rightarrow t\bar{t} \rightarrow W^\mp b \Delta^\pm b$ is simulated for various m_{Δ^\pm} in the 100–160 GeV range. For the reconstruction and selection of physics objects, namely leptons (electrons and muons) and jets (including b -tagged jets), we closely follow the respective CMS and ATLAS analyses. We then

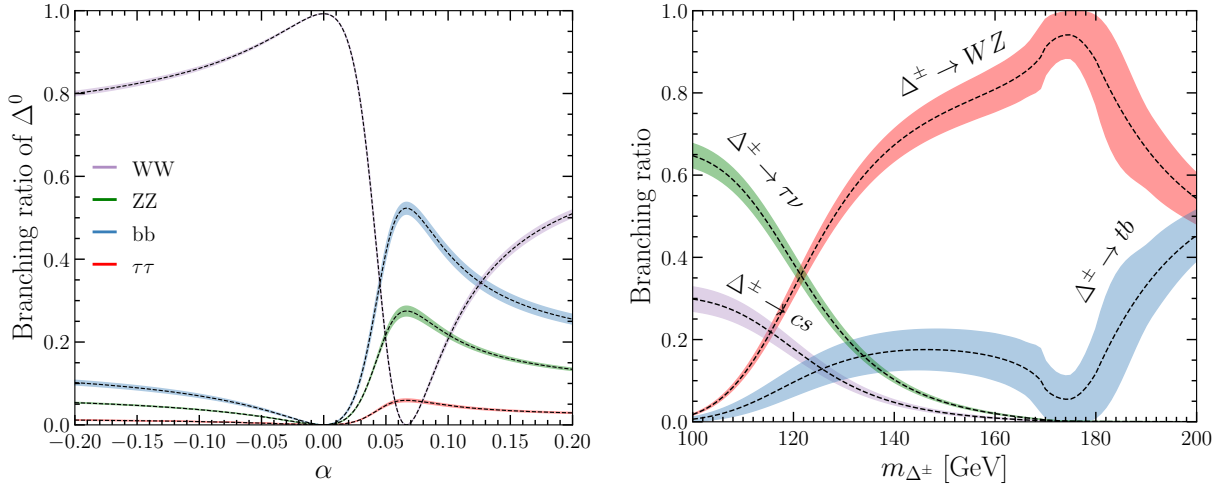


Fig. 2: Left: Dominant branching ratios of Δ^0 , including the uncertainties estimated from Ref. [40], and $m_{\Delta^0} = 150$ GeV. Right: Dominant branching ratios of Δ^\pm , including the uncertainties estimated from Ref. [40], as a function of its mass. We have assumed $\alpha \approx 0$.

performed a chi-square analysis with the available binned observed data, SM prediction, and the NP contribution, assuming $\text{Br}(t \rightarrow \Delta^\pm b) \times \text{Br}(\Delta^\pm \rightarrow WZ)$ as the NP signal strength and obtained the model-independent limit on $\text{Br}(t \rightarrow \Delta^\pm b) \times \text{Br}(\Delta^\pm \rightarrow WZ)$ (see left panel of Figure 2 of Ref. [41]).

3 Model Description: The Real Higgs Triplet Model (Δ SM)

We consider the extension of the SM scalar sector by a real $SU(2)_L$ Higgs triplet with zero hypercharge ($Y = 0$), commonly referred to as the Δ SM [20, 21, 42–47]. The model introduces a CP-even neutral scalar (Δ^0) and a charged Higgs bosons (Δ^\pm).

The SM Higgs doublet is represented by Φ and the real triplet by Δ , can be decomposed as

$$\Phi = \begin{pmatrix} \phi^+ \\ \frac{1}{\sqrt{2}}(v_\phi + h_\phi^0 + iG^0) \end{pmatrix}, \quad (9)$$

$$\Delta = \frac{1}{2} \begin{pmatrix} v_\Delta + h_\Delta^0 & \sqrt{2}\Delta^+ \\ \sqrt{2}\Delta^- & -(v_\Delta + h_\Delta^0) \end{pmatrix}. \quad (10)$$

The tree-level scalar potential is given by

$$V = -\mu_\phi^2 \Phi^\dagger \Phi + \frac{\lambda_\phi}{4} (\Phi^\dagger \Phi)^2 - \mu_\Delta^2 \text{Tr}(\Delta^\dagger \Delta) + \frac{\lambda_\Delta}{4} [\text{Tr}(\Delta^\dagger \Delta)]^2 + A \Phi^\dagger \Delta \Phi + \lambda_{\phi\Delta} \Phi^\dagger \Phi \cdot \text{Tr}(\Delta^\dagger \Delta), \quad (11)$$

where all parameters are taken to be real, such that the potential is CP conserving. Note that in the limit $A \rightarrow 0$,

the potential possesses a global $O(4)_\Phi \times O(3)_\Delta$ symmetry and the discrete $Z_{2,\Delta}(\Delta \rightarrow -\Delta)$ symmetry. Therefore, a non-zero A , corresponding to $A\Phi^\dagger \Delta \Phi$ term, leads to a soft breaking of this symmetry such that small values of it are natural in the t' Hooft sense and governs the mixing between the doublet and triplet scalars [41].

After electroweak symmetry breaking, the physical scalar spectrum consists of the SM-like Higgs boson h , identified with the 125 GeV scalar, the neutral triplet-like scalar Δ^0 , and the charged scalars Δ^\pm . The masses of the triplet-like scalars are approximately

$$m_{\Delta^0}^2 \approx \frac{1}{2} \lambda_\Delta v_\Delta^2 + \frac{A v_\phi^2}{4 v_\Delta}, \quad (12)$$

$$m_{\Delta^\pm}^2 = \frac{A(v_\phi^2 + 4v_\Delta^2)}{4v_\Delta}, \quad (13)$$

in an expansion in v_Δ/v . The mixing angle α between the neutral scalars, defined as $\tan \alpha \approx \frac{4v_\Delta}{v}$, governs the deviation of Higgs couplings from their SM expectations and is constrained by precision Higgs measurements.

The triplet vacuum expectation value v_Δ contributes at tree level only to the W boson mass but not to the Z mass, leading to a deviation in the ρ -parameter given by

$$\rho_{\text{tree}} \approx 1 + \frac{4v_\Delta^2}{v^2}, \quad (14)$$

where $v^2 = v_\phi^2 + 4v_\Delta^2 \approx (246 \text{ GeV})^2$. Electroweak precision data tightly constrain this contribution, requiring $v_\Delta < \mathcal{O}(1 \text{ GeV})$. Note that the model predicts a positive shift in the W -boson mass, potentially explaining the recently reported experimental deviation from the SM expectation. Again the small mixing resulting from the $\mathcal{O}(1 \text{ GeV})$

triplet vev, makes the doublet and triplet mostly decoupled and hence therefore free of tree-level flavor-changing effects [24].

To ensure theoretical consistency, the parameter space is subject to several constraints. Vacuum stability requires the scalar potential to be bounded from below in all field directions, which imposes the conditions

$$\lambda_\phi > 0, \quad \lambda_\Delta > 0, \quad \sqrt{2}\lambda_{\phi\Delta} + \sqrt{\lambda_\phi\lambda_\Delta} > 0. \quad (15)$$

Perturbative unitarity bounds on all $2 \rightarrow 2$ scalar scattering amplitudes further constrain the quartic couplings, for instance,

$$|\lambda_\phi| \leq 2\kappa\pi, \quad |\lambda_\Delta| \leq 2\kappa\pi, \quad |\lambda_{\phi\Delta}| \leq \kappa\pi, \quad \text{with } \kappa = 16. \quad (16)$$

These conditions restrict the allowed mass splitting between Δ^0 and Δ^\pm to be only a few GeV once the bound on v_Δ from the W mass is taking into account.

Note that since the triplet does not couple to the SM fermions at the renormalizable level, so the Yukawa Lagrangian remains SM-like and deviations of the SM Higgs couplings to fermion originate from mixing only.

Since v_Δ and thus the mixing with the SM Higgs is small, the triplet-like scalars are primarily produced at the LHC via Drell-Yan processes [48],

$$q\bar{q} \rightarrow Z^*/\gamma^* \rightarrow \Delta^\pm \Delta^\mp, \quad q\bar{q}' \rightarrow W^{\pm*} \rightarrow \Delta^0 \Delta^\pm. \quad (17)$$

The neutral scalar Δ^0 predominantly decays into WW , with loop-induced channels such as $\gamma\gamma$ and $Z\gamma$ becoming relevant when the scalar is nearly degenerate with Δ^\pm . In Fig 2, we show the branching ratios of Δ^0 to various possible modes with respect to the scalar mixing angle α . For $\alpha \simeq 0$, the $\text{Br}(\Delta^0 \rightarrow WW)$ is 100%, whereas when $\text{Br}(\Delta^0 \rightarrow WW) \approx 0$ (which corresponds to $\alpha \simeq 0.065$), other decay mode dominates. From the Fig 2, at $m_{\Delta^\pm} = 150$ GeV and $\text{Br}(\Delta^0 \rightarrow WW) \approx 0$, the dominant decays modes are bb, ZZ with $\text{Br}(\Delta^0 \rightarrow bb) \approx 50\%$ and $\text{Br}(\Delta^0 \rightarrow ZZ) \approx 30\%$ respectively.

The charged scalar Δ^\pm typically decays to $WZ, \tau\nu$, or tb , depending on its masses. In Fig. 2, we have shown the branching ratios of Δ^\pm as a function of its mass.

In Fig. 2, the uncertainties are estimated by propagating the errors on the $\tau\tau, c\bar{c}, t\bar{t}, WW$ and ZZ decays of a hypothetical SM-like Higgs with mass m_{Δ^0} and m_{Δ^\pm} , respectively, as reported in the CERN Yellow Report [40].

The phenomenological implications in di-photon final states were examined in Refs. [22–24], finding that the ΔSM can account for the excess at 152 GeV. We also have recasted $t\bar{t}Z$ analyses of LHC [31,32] to search for signs of charged Higgs bosons and set novel limits on the product of branching fractions $\text{Br}(t \rightarrow \Delta^\pm b) \times \text{Br}(\Delta^\pm \rightarrow WZ)$, which when translated onto the ΔSM shows a $\sim 2\sigma$ pref-

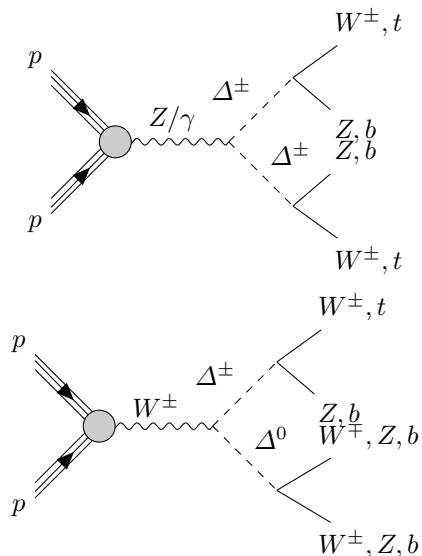


Fig. 3: Feynman diagram for the Drell-Yan production of triplet scalars $pp \rightarrow \Delta^\pm \Delta^\mp, \Delta^\pm \Delta^0$ further decaying to W, Z , which will contribute to SM VVV processes, where $V = W, Z$.

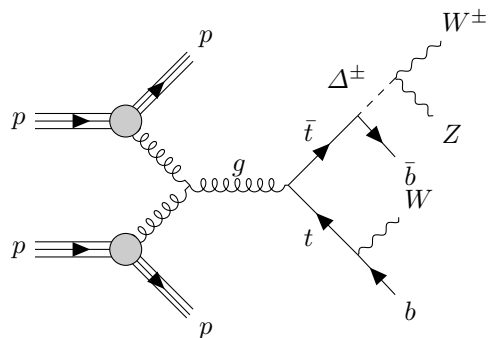


Fig. 4: Representative Feynman diagram for $pp \rightarrow t\bar{t}$ with $t \rightarrow \Delta^\pm b$ and $\Delta^\pm \rightarrow W^\pm Z$, leading to a $t\bar{t}Z$ -like SM signature and tWZ -like SM signature with additional b -jets.

erence, see Ref [41]. Multi-lepton searches we studied in Refs. [16, 24], finding that the scalar triplet is consistent with data. Here we want to consider these channels in more detail recasting the multi-boson searches discussed above.

4 Results

In the ΔSM we have two different processes which lead to the production of EW gauge bosons and thus multiple leptons. First, there is the Drell-Yan production of $\Delta^\pm \Delta^0$ and $\Delta^\pm \Delta^\mp$ shown in Fig. 3. This effect is unavoidable and will be discussed in the next subsection. In addition, we have the process $pp \rightarrow t\bar{t} \rightarrow \Delta^\pm bW\bar{b}$ which can happen in our

Analysis	$\mu_{\text{EXP}} = \sigma_{\text{EXP}}/\sigma_{\text{SM}}$	$\mu_{\Delta^\pm\Delta^0}$	$\mu_{\Delta^\pm\Delta^\mp}$	$\mu_{t\bar{t}}$	μ_{NP}
		$WW = 100\%(WW = 0\%)$			
VVZ [26]	1.43 ± 0.29	0.33(0.15)	0.19	0	0.52(0.34)
WWW [29]	1.61 ± 0.25	0.76(0.07)	0.14	0	0.90(0.21)
WWZ (Run 2) [27]	0.52 ± 0.52	0.86(0.63)	0.64	0	1.50(1.27)
WWZ (Run 3) [27]	1.91 ± 1.15	0.99(0.68)	0.53	0	1.52(1.21)
tWZ (Run 2) [30]	1.82 ± 0.38	0.20(0.41)	0.25	0.93	0.93(1.05)
tWZ (Run 3) [30]	1.64 ± 0.52	0.19(0.38)	0.22	0.73	0.79(0.90)

Table 2: Predicted NP signal strength relative to the SM (μ_{NP}), along with the contribution from the relevant NP processes: $pp \rightarrow W^+ \rightarrow \Delta^\pm\Delta^0$ ($\mu_{\Delta^\pm\Delta^0}$), $pp \rightarrow \gamma^*, Z^* \rightarrow \Delta^\pm\Delta^\mp$ ($\mu_{\Delta^\pm\Delta^\mp}$) and $pp \rightarrow t\bar{t} \rightarrow \Delta^\pm bWb$ ($\mu_{t\bar{t}}$). The NP contribution from $t\bar{t}$ channel for tWZ is normalized to $\text{Br}(t \rightarrow \Delta^\pm b) = 10^{-3}$.

setup with $m_{\Delta^\pm} \approx 150$ GeV. However, this rate depends on v_Δ and thus involves an additional free parameter.

For the simulation, we followed the same chain of packages as for the SM. Furthermore, to correct for the effects of our fast simulation, we will always consider the ratio of NP over SM, i.e. $\mu_{\text{NP}} = \sigma_{\Delta\text{SM}}^{\text{vis}}/\sigma_{\text{SM}}^{\text{vis}}$, where vis stands for the visible cross section (i.e. after acceptance, efficiency and cuts).

Therefore, this χ^2 function can be constructed as

$$\chi^2 = \left(\frac{\mu_{\text{EXP}} - (1 + x \times \mu_{\text{NP}})}{\Delta\mu} \right)^2. \quad (18)$$

Here, we introduced the fitting parameter x (x is not a physical parameter of the model, rather an effective scaling factor corresponding to the new physics signal strength) such that the NP signal strength can be varied for illustrational purposes. The ΔSM scenario corresponds to $x = 1$.

4.1 $pp \rightarrow \Delta^\pm\Delta^0$ and $pp \rightarrow \Delta^\pm\Delta^\mp$

Fig. 3, shows the DY production of the triplet scalars $pp \rightarrow \Delta^\pm\Delta^0, \Delta^\pm\Delta^\mp$ with their main decay modes into gauge bosons. While the branching ratios of Δ^\pm are determined as a function of the mass only, the dominant decay modes of Δ^0 depend in addition on the mixing angle α with the SM Higgs (see Fig. 2). Therefore, we will consider two limiting case for the latter: 1) $\text{Br}(\Delta^\pm \rightarrow WW) \approx 100\%$ and 2) $\text{Br}(\Delta^\pm \rightarrow WW) \approx 0\%$, which leads to $(\Delta^\pm \rightarrow ZZ) \approx 30\%$ and $(\Delta^\pm \rightarrow bb) \approx 50\%$.

VVZ: The NP contribution to the SM $pp \rightarrow VVZ$ process, where $V = W, Z$, comes from the $\Delta^\pm\Delta^\mp$ channel and the $\Delta^\pm\Delta^0$ channel, the latter depending on the $\text{Br}(\Delta^0 \rightarrow WW)$. The visible NP cross section originating from the $pp \rightarrow \Delta^\mp\Delta^\pm$ is 0.57 fb. The process $pp \rightarrow \Delta^0\Delta^\pm$ contribution is 0.99 (0.45) fb for $\text{Br}(\Delta^0 \rightarrow WW) = 100\%$ (0%). This results in a NP signal strength relative to the SM ($\mu_{\text{NP}}^{\text{VVZ}}$) of 0.52(0.34) for $\text{Br}(\Delta^0 \rightarrow WW) = 100\%$ (0%).

WWW: The DY pair production NP contribution to the $pp \rightarrow WWW$ process is 0.27 fb from $pp \rightarrow \Delta^\mp\Delta^\pm$ and

1.47(0.14) fb from $pp \rightarrow \Delta^0\Delta^\pm$ with $\text{Br}(\Delta^0 \rightarrow WW) = 100\%$ (0%). The NP signal strength relative to the SM ($\mu_{\text{NP}}^{\text{WWW}}$) for $\text{Br}(\Delta^0 \rightarrow WW) = 100\%$ (0%) is 0.90(0.21).

WWZ: The NP contribution to the SM $pp \rightarrow WWZ$ process for Run 2 is 0.04 fb from $pp \rightarrow \Delta^\mp\Delta^\pm$ and 0.053 (0.039) fb from $pp \rightarrow \Delta^0\Delta^\pm$ with $\text{Br}(\Delta^0 \rightarrow WW) = 100\%$ (0%) and for Run 3 the contributions are 0.03 fb and 0.057(0.040) fb, respectively. The NP signal strength relative to the SM ($\mu_{\text{NP}}^{\text{WWZ}}$) for $\text{Br}(\Delta^0 \rightarrow WW) = 100\%$ (0%) for Run 2 is 1.50(1.27) and for Run 3 is 1.52(1.21).

tWZ: The DY processes $pp \rightarrow \Delta^\mp\Delta^\pm$ and $pp \rightarrow \Delta^\mp\Delta^0$ can also contribute to SM process $pp \rightarrow tWZ$, which results in a $WWZb$ final state. From $\Delta^\mp\Delta^\pm$ process, when one of the Δ^\pm decays to $t^*b(Wbb)$ and others decays to WZ , we can have $WWZb$ with additional b -jets, where the $\text{Br}(\Delta^\pm \rightarrow WZ) \approx 75\%$, and $\text{Br}(\Delta^\pm \rightarrow tb) \approx 17\%$ (see Fig. 2). Similarly, from $\Delta^\mp\Delta^0$ process, we can also get tWZ like signature with additional jets when $\Delta^\pm \rightarrow WZ, t^*b$ and $\Delta^0 \rightarrow WW, ZZ, bb$. The $\Delta^\mp\Delta^0$ contribution is considered in two extreme situations depending upon the $\text{Br}(\Delta^0 \rightarrow WW)$: $WW = 100\%$ and $WW = 0\%$ ($ZZ \approx 30\%$, and $bb \approx 50\%$). The Run 2 $\Delta^\mp\Delta^\pm$ contribution to SM tWZ process is 0.09 fb and $\Delta^\pm\Delta^0$ contribution for $WW = 100\%$ ($WW = 0\%$) is 0.071(0.14) fb. Similarly for Run 3 the contributions are 0.076 fb and 0.069(0.13) fb, respectively.

ttZ: Similar to the tWZ process, the $pp \rightarrow \Delta^\pm\Delta^\mp$ could contribute to ttZ like-final states. However, in this case, the SM cross section is significantly larger than the tWZ cross section and the efficiency of the cuts for the NP signal $\Delta^\pm\Delta^\mp \rightarrow WZt^*b$ is lower: We found that the relative NP signal strength compared to the SM is below 1%, both for ATLAS and CMS. Therefore, we can neglect the Drell-Yan contribution to the ttZ channel and will only include the effect of $pp \rightarrow t\bar{t} \rightarrow \Delta^\pm bWb$ for which we can directly reuse the results of Ref. [41] (see next subsection).

Drell-Yan combination: The resulting χ^2 as a function of the fitting parameter x is given in Fig. 5, where we have assumed $\text{Br}(t \rightarrow \Delta^\pm b) = 0$ and disregarded the small effect in the ttZ signal region. In left (right)

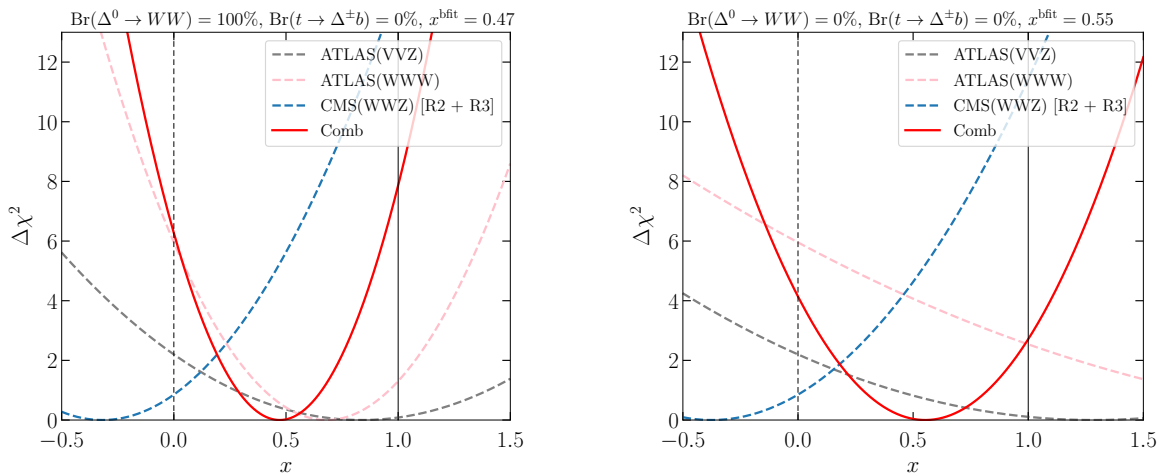


Fig. 5: Left: Chi-square distribution as a function of the fitting parameter x for the tri-boson channels (excluding tWZ). We consider for $\text{Br}(\Delta^0 \rightarrow WW) = 100\%$ and $\text{Br}(t \rightarrow \Delta^\pm b) = 0\%$. The red line represents the combined chi square distribution, with $\chi_{\text{comb}}^2(x=0) = 15.8$, $\chi_{\text{comb}}^2(\text{min}) = 9.5$, and deviation w.r.t. the SM: $\sqrt{\Delta\chi_{\text{comb}}^2(x=0)} \approx 2.5\sigma$. Right: Same for $\text{Br}(\Delta^0 \rightarrow WW) = 0\%$ resulting in $\chi_{\text{comb}}^2(\text{min}) = 11.6$ corresponding to $\sqrt{\Delta\chi_{\text{comb}}^2(x=0)} \approx 2\sigma$.

panel of Fig. 5, we show the results for $\text{Br}(\Delta^0 \rightarrow WW = 100\%)$ ($\text{Br}(\Delta^0 \rightarrow WW = 0\%)$). At $x = 0$, the combined chi square (χ_{comb}^2) is $\chi_{\text{comb}}^2(x=0) = 15.74$, and the minimum of the χ_{comb}^2 for 100%(0%) WW branching is $\chi_{\text{comb}}^2(x_{\text{min}}) = 9.47(11.6)$ for best fit value of the fitting parameter $x^{\text{b-fit}} = 0.47(0.55)$ respectively. Therefore, we have a $\Delta\chi^2 = \chi_{\text{comb}}^2(x=0) - \chi_{\text{comb}}^2(\text{min}) = 6.27(4.14)$ corresponding to $\sqrt{\Delta\chi_{\text{comb}}^2(x=0)} = 2.5\sigma(2.03\sigma)$, respectively. However, the ΔSM predicts $x = 1$, with a χ^2 of 17.34(14.31), such that the model is consistent with data but not preferred over the SM hypothesis.

4.2 $pp \rightarrow t\bar{t} \rightarrow \Delta^\pm bWb$

Fig. 4 shows the contribution from the ΔSM , which contributes to the tWZ and ttZ analyses. As we can neglect the effect of the Drell-Yan production in the ttZ channel, we can directly reuse the results of Ref. [41]:

$$\text{Br}(\Delta^\pm \rightarrow W^\pm Z) = (0.13 \pm 0.064)\% \quad (\text{CMS}), \quad (19)$$

and

$$\text{Br}(\Delta^\pm \rightarrow W^\pm Z) = (0.054 \pm 0.037)\% \quad (\text{ATLAS}). \quad (20)$$

In the tWZ signal region, we have the contribution from the Drell-Yan production discussed previously and the effect of $pp \rightarrow t\bar{t} \rightarrow \Delta^\pm bWb$ (see Fig. 4). The obtained NP signal strengths for the $t\bar{t}$ process ttZ Run 2 (Run 3) is

$$\mu_{t\bar{t}}^{ttZ} = 0.93(0.73) \times \text{Br}(t \rightarrow \Delta^\pm b)/10^{-3}. \quad (21)$$

We can thus perform the combined fit to x and $\text{Br}(t \rightarrow \Delta^\pm b)$ in Fig. 6 for $\text{Br}(\Delta^0 \rightarrow WW) = 100\%$ shown in the left and for $\text{Br}(\Delta^0 \rightarrow WW) = 0\%$ shown in the right panel. From the left with 100% WW mode, we get best fit values as $\text{Br}^{\text{bfit}}(t \rightarrow \Delta^\pm b) = 0.068\%$ and $x^{\text{bfit}} = 0.36$. Similarly from the left with 0% WW decay of Δ^0 , we get best fit values as $\text{Br}^{\text{bfit}}(t \rightarrow \Delta^\pm b) = 0.07\%$ and $x^{\text{bfit}} = 0.21$. This corresponds to a preference over the SM hypothesis of 2.97σ and 2.47σ assuming 2 degree of freedom (x and $\text{Br}(t \rightarrow \Delta^\pm b)$), respectively. In this case, the ΔSM with $x = 1$ shows a slight preference over the SM of $1.3\sigma(1.6\sigma)$ and $\text{Br}=0.053\%$ (0.043%).

5 Conclusion

Motivated by the long-standing multi-lepton anomalies at the LHC, we previously argued for the presence of an additional scalar state with a mass around 150 GeV. Subsequent LHC measurements in fact show indications for a narrow resonance with 152 ± 1 GeV which can be partially explained with the ΔSM model.

In this framework, the same dynamics that account for the observed $\gamma\gamma + X$ signatures imply correlated effects in triboson production. In particular, the model predicts an enhancement in VVV rates data. While there are indications for enhanced tri-boson cross sections, the ΔSM predicts a higher signal strength than the currently preferred central value, resulting in an inclusive result. Exploiting the available Run 2 measurements, we reported the first hint of the predicted excess in VVV production, with a significance of 2.6σ . With the increased luminosity and improved systematics expected from Run 3, the LHC

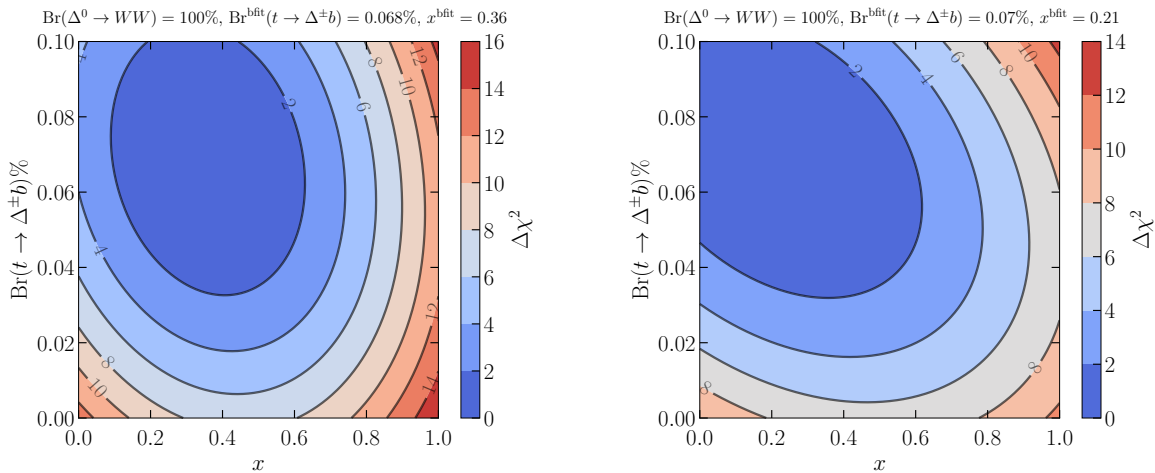


Fig. 6: Left: χ^2 contours as a function of x and $\text{Br}(t \rightarrow \Delta^{\pm}b)$ assuming $\text{Br}(\Delta^0 \rightarrow WW) = 100\%$. We find a preference for NP of $\approx 3\sigma$ (for 2DoF). Same for $\text{Br}(\Delta^0 \rightarrow WW) = 0\%$ resulting in $\approx 2.5\sigma$. In the above chi-square distribution, $x = 0$ and $\text{Br}(t \rightarrow \Delta^{\pm}b) = 0$ corresponds to the SM model, while $x = 1$ corresponds to the real triplet model.

program should be able to decisively test this prediction. Confirmation of the triboson excess would provide an independent and complementary validation of the emerging picture of new bosonic degrees of freedom in the LHC data, and would strongly motivate dedicated differential studies and global fits to pin down the underlying electroweak representation and couplings.

Finally, we need to note that the charged component of the triplet can be scrutinised in great detail at future electron-positron colliders [25]. This includes precise measurements of the masses, and exploration of couplings and quantum numbers with precision that cannot be attained at high-energy hadron colliders.

A Appendix

This section contains the cut-flows performed for the analysis considered in the article, see Table. [1, 2]. The cut flows for all the analysis is shown as, VVZ : Table. [3,4,5], WWZ (Run 2 and Run 3): Table. [6, 7], WWW : Table. [8, 9], and tWW (Run 2 and Run 3): Table. [10, 11].

References

1. **ATLAS** Collaboration, G. Aad et al., “Observation of a new particle in the search for the Standard Model Higgs boson with the ATLAS detector at the LHC,” *Phys. Lett. B* **716** (2012) 1–29, [arXiv:1207.7214 \[hep-ex\]](#).
2. **CMS** Collaboration, S. Chatrchyan et al., “Observation of a New Boson at a Mass of 125 GeV with the CMS Experiment at the LHC,” *Phys. Lett. B* **716** (2012) 30–61, [arXiv:1207.7235 \[hep-ex\]](#).
3. A. Crivellin and B. Mellado, “Anomalies in particle physics and their implications for physics beyond the standard model,” *Nature Rev. Phys.* **6** no. 5, (2024) 294–309, [arXiv:2309.03870 \[hep-ph\]](#).
4. O. Fischer et al., “Unveiling hidden physics at the LHC,” *Eur. Phys. J. C* **82** no. 8, (2022) 665, [arXiv:2109.06065 \[hep-ph\]](#).
5. S. von Buddenbrock, N. Chakrabarty, A. S. Cornell, D. Kar, M. Kumar, T. Mandal, B. Mellado, B. Mukhopadhyaya, R. G. Reed, and X. Ruan, “Phenomenological signatures of additional scalar bosons at the LHC,” *Eur. Phys. J. C* **76** no. 10, (2016) 580, [arXiv:1606.01674 \[hep-ph\]](#).
6. S. von Buddenbrock, A. S. Cornell, A. Fadol, M. Kumar, B. Mellado, and X. Ruan, “Multi-lepton signatures of additional scalar bosons beyond the Standard Model at the LHC,” *J. Phys. G* **45** no. 11, (2018) 115003, [arXiv:1711.07874 \[hep-ph\]](#).
7. Y. Hernandez, M. Kumar, A. S. Cornell, S.-E. Dahbi, Y. Fang, B. Lieberman, B. Mellado, K. Monnakgotla, X. Ruan, and S. Xin, “The anomalous production of multi-lepton and its impact on the measurement of Wh production at the LHC,” *Eur. Phys. J. C* **81** no. 4, (2021) 365, [arXiv:1912.00699 \[hep-ph\]](#).
8. S. Buddenbrock, A. S. Cornell, Y. Fang, A. Fadol Mohammed, M. Kumar, B. Mellado, and K. G. Tomiwa, “The emergence of multi-lepton anomalies at the LHC and their compatibility with new physics at the EW scale,” *JHEP* **10** (2019) 157, [arXiv:1901.05300 \[hep-ph\]](#).
9. **ATLAS** Collaboration, G. Aad et al., “Search for dark matter in events with missing transverse momentum and a Higgs boson decaying into two photons in pp collisions at $\sqrt{s} = 13$ TeV with the ATLAS detector,” *JHEP* **10** (2021) 013, [arXiv:2104.13240 \[hep-ex\]](#).

Cut	$\Delta^0 \Delta^\pm$	$\Delta^0 \Delta^\pm$	$\Delta^\mp \Delta^\pm$	SM VVZ
	WW(100%)	WW(0%)		
≥ 3 leptons	537	185	287	655
Exactly 3 leptons and 1 jet	430	145	238	539
Lepton p_T cuts (27,15,15)	327	112	182	476
≥ 1 OSSF pair	290	110	177	469
All OSSF $m_{\ell\ell} \geq 12\text{GeV}$	277	106	170	466
Z mass window $ m_{\ell\ell} - M_Z < 20\text{ GeV}$	132	69	88	445
$1.37 < \eta_\ell < 1.52$	132	69	87	443
≥ 1 jet with $p_T > 20\text{ GeV}$, b -jet veto	111	48	63	366
3 ℓ -1j	26	12	14	77
3 ℓ -2j (in V)	31	13	21	123
3 ℓ -2j (out V)	54	23	28	165

Table 3: Cutflow table VVZ (ATLAS) [26] 3 ℓ SR.

Cut	$\Delta^0 \Delta^\pm$	$\Delta^0 \Delta^\pm$	$\Delta^\mp \Delta^\pm$	SM VVZ
	WW(100%)	WW(0%)		
= 4 leptons	57	26	34	71
Lepton p_T cuts (30,15,8,6)	57	25	33	68
≥ 1 OSSF pair	56	25	33	68
All OSSF $m_{\ell\ell} \geq 12\text{GeV}$	52	23	30	66
Z mass window $ m_{\ell\ell} - M_Z < 20\text{ GeV}$	31	19	19	66
$p_T^{miss} > 10\text{ GeV}$, b -jet veto	26	13	15	55
4 ℓ -DF	12	2	6	20
4 ℓ -SF (in V)	3	2	2	18
4 ℓ -SF (out V)	12	9	7	17

Table 4: Cutflow table VVZ (ATLAS) [26] 4 ℓ SR.

Cut	$\Delta^0 \Delta^\pm$	$\Delta^0 \Delta^\pm$	$\Delta^\mp \Delta^\pm$	SM VVZ
	WW(100%)	WW(0%)		
≥ 5 leptons	4.89	4.64	3.43	2.97
≥ 2 OSSF pair	1.49	1.96	1.48	2.97
b -jet veto	1.49	1.76	1.43	2.71

Table 5: Cutflow table VVZ (ATLAS) [26] 5 ℓ SR.

Cut	$\Delta^0 \Delta^\pm$	$\Delta^0 \Delta^\pm$	$\Delta^\mp \Delta^\pm$	SM WWZ
	WW(100%)	WW(0%)		
= 4 leptons	65.88	28.65	35.6	24.38
$p_T(\ell_1) > (25, 15, 10, 10)$	65.36	28.45	35.4	24.38
b -jet veto	13.51	9.36	8.85	13.36
OF	5.55	2.93	3.23	5.74
SF	1.78	2.46	2.24	2.64

Table 6: Cutflow table WWZ (CMS) [27] 4 ℓ SR for Run 2.

Cut	$\Delta^0 \Delta^\pm$	$\Delta^0 \Delta^\pm$	$\Delta^\mp \Delta^\pm$	SM WWZ
	WW(100%)	WW(0%)		
= 4 leptons	27.01	12.74	15.41	10.84
$p_T(\ell_1) > (25, 15, 10, 10)$	26.92	12.73	15.32	10.84
b -jet veto	5.32	3.93	3.58	6.25
OF	2.4	1.34	1.38	2.48
SF	1.13	1.11	1.1	1.12

Table 7: Cutflow table WWZ (CMS) [27] 4 ℓ SR for Run 3.

Cut	$\Delta^0\Delta^\pm$	$\Delta^0\Delta^\pm$	$\Delta^\mp\Delta^\pm$	SM WWW
	$WW(100\%)$	$WW(0\%)$		
= 2 leptons	2296	564	863	2931
Leptons with Same charge	643	87	143	838
≥ 1 jet, b -jet veto	362	46	81	498
$p_T(\ell_1) > 27, 40 \text{ GeV} < m_{\ell\ell} < 400 \text{ GeV}$	322	38	63	432
$m_{jj} < 160 \text{ GeV}$	179	21	37	250
$ee - mode$	14	2	3	30
$e\mu - mode$	89	11	18	121
$\mu\mu - mode$	58	5	11	79

Table 8: Cutflow table WWW (ATLAS) [29] 2ℓ SR.

Cut	$\Delta^0\Delta^\pm$	$\Delta^0\Delta^\pm$	$\Delta^\mp\Delta^\pm$	SM WWW
	$WW(100\%)$	$WW(0\%)$		
= 3 leptons	307	103	165	174
$p_T(\ell_1) > 27$	306	103	164	174
b -jet veto and no-OSSF leptons	35	2	5	38

Table 9: Cutflow table WWW (ATLAS) [29] 3ℓ SR.

Cut	NP1	NP2	$WW(100\%)$	$WW(0\%)$	SM tWZ
	$pp \rightarrow t\bar{t}$ $t \rightarrow \Delta^\pm b$ (0.01%), $\bar{t} \rightarrow Wb$	$pp \rightarrow \Delta^\pm\Delta^\mp$ $\Delta^\pm \rightarrow tb$ $\Delta^\mp \rightarrow WZ$	$pp \rightarrow \Delta^0\Delta^\mp$ $\Delta^\pm \rightarrow tb, WZ$ $\Delta^0 \rightarrow WW$	$pp \rightarrow \Delta^0\Delta^\mp$ $\Delta^\pm \rightarrow tb, WZ$ $\Delta^0 \rightarrow bb, ZZ$	
at least 3 leptons	80.1	309.56	580.9	291.69	198.91
$p_T(\ell_1, \ell_2) > (25, 15) \text{ GeV}$	78.53	303.63	568.02	285.48	197.85
at least 1 OSSF with $ m_{\ell\ell} - m_Z < 15 \text{ GeV}$	9.25	86.57	123.18	95.53	99.51
= $3\ell, 2j$, at least 1 b -jet	3.66	10.51	7.96	16.3	41.59
= 4ℓ , at least 1 b -jet	0.87	1.87	1.89	3.67	7.0

Table 10: Cutflow table tWZ (CMS) [30] for Run 2.

Cut	NP1	NP2	$WW(100\%)$	$WW(0\%)$	SM tWZ
	$pp \rightarrow t\bar{t}$ $t \rightarrow \Delta^\pm b$ (0.01%), $\bar{t} \rightarrow Wb$	$pp \rightarrow \Delta^\pm\Delta^\mp$ $\Delta^\pm \rightarrow tb$ $\Delta^\mp \rightarrow WZ$	$pp \rightarrow \Delta^0\Delta^\mp$ $\Delta^\pm \rightarrow tb, WZ$ $\Delta^0 \rightarrow WW$	$pp \rightarrow \Delta^0\Delta^\mp$ $\Delta^\pm \rightarrow tb, WZ$ $\Delta^0 \rightarrow bb, ZZ$	
at least 3 leptons	28.31	114.17	201.64	108.75	86.6
$p_T(\ell_1, \ell_2) > (25, 15) \text{ GeV}$	28.07	113.82	200.84	108.35	86.6
OSSF with $ m_{\ell\ell} - m_Z < 15 \text{ GeV}$	3.53	33.28	43.34	37.1	43.57
= $3\ell, 2j$, at least 1 b -jet	1.33	4.19	3.72	6.5	18.43
= 4ℓ , at least 1 b -jet	0.24	0.54	0.47	1.5	2.91

Table 11: Cutflow table tWZ (CMS) [30] for Run 3.

10. **ATLAS** Collaboration, G. Aad et al., “Model-independent search for the presence of new physics in events including $H \rightarrow \gamma\gamma$ with $\sqrt{s} = 13 \text{ TeV}$ pp data recorded by the ATLAS detector at the LHC,” *JHEP* **07** (2023) 176, [arXiv:2301.10486](#) [[hep-ex](#)].
11. **CMS** Collaboration, A. M. Sirunyan et al., “Search for the decay of a Higgs boson in the $\ell\ell\gamma$ channel in proton-proton collisions at $\sqrt{s} = 13 \text{ TeV}$,” *JHEP* **11** (2018) 152, [arXiv:1806.05996](#) [[hep-ex](#)].
12. **CMS** Collaboration, A. Tumasyan et al., “Search for Higgs boson decays to a Z boson and a photon in proton-proton collisions at $\sqrt{s} = 13 \text{ TeV}$,” *JHEP* **05** (2023) 233, [arXiv:2204.12945](#) [[hep-ex](#)].
13. **CMS** Collaboration, A. Tumasyan et al., “Measurements of the Higgs boson production cross section and couplings in the W boson pair decay channel in proton-proton collisions at $\sqrt{s} = 13 \text{ TeV}$,” *Eur. Phys. J. C* **83** no. 7, (2023) 667, [arXiv:2206.09466](#) [[hep-ex](#)].
14. **ATLAS** Collaboration, G. Aad et al., “Measurements of Higgs boson production by gluon-gluon fusion and vector-boson fusion using $H \rightarrow WW^* \rightarrow \nu\mu\nu$ decays in pp collisions at $\sqrt{s} = 13 \text{ TeV}$ with the ATLAS detector,”

- Phys. Rev. D* **108** (2023) 032005, [arXiv:2207.00338 \[hep-ex\]](#).
15. G. Coloretti, A. Crivellin, S. Bhattacharya, and B. Mellado, “Searching for low-mass resonances decaying into W bosons,” *Phys. Rev. D* **108** no. 3, (2023) 035026, [arXiv:2302.07276 \[hep-ph\]](#).
 16. A. Crivellin, Y. Fang, O. Fischer, S. Bhattacharya, M. Kumar, E. Malwa, B. Mellado, N. Rapheeha, X. Ruan, and Q. Sha, “Accumulating evidence for the associated production of a new Higgs boson at the LHC,” *Phys. Rev. D* **108** no. 11, (2023) 115031, [arXiv:2109.02650 \[hep-ph\]](#).
 17. S. Bhattacharya, B. Lieberman, M. Kumar, A. Crivellin, Y. Fang, R. Mazini, and B. Mellado, “Emerging Excess Consistent with a Narrow Resonance at 152 GeV in High-Energy Proton-Proton Collisions,” [arXiv:2503.16245 \[hep-ph\]](#).
 18. CMS Collaboration, A. Tumasyan et al., “A portrait of the Higgs boson by the CMS experiment ten years after the discovery,” *Nature* **607** no. 7917, (2022) 60–68, [arXiv:2207.00043 \[hep-ex\]](#). [Erratum: *Nature* 623, (2023)].
 19. ATLAS Collaboration, G. Aad et al., “Higgs boson production cross-section measurements and their EFT interpretation in the 4ℓ decay channel at $\sqrt{s}=13$ TeV with the ATLAS detector,” *Eur. Phys. J. C* **80** no. 10, (2020) 957, [arXiv:2004.03447 \[hep-ex\]](#). [Erratum: *Eur.Phys.J.C* 81, 29 (2021), Erratum: *Eur.Phys.J.C* 81, 398 (2021)].
 20. D. A. Ross and M. J. G. Veltman, “Neutral currents and the Higgs mechanism,” *Nucl. Phys. B* **95** (1975) 135–147.
 21. J. F. Gunion, R. Vega, and J. Wudka, “Higgs triplets in the standard model,” *Phys. Rev. D* **42** (1990) 1673–1691.
 22. S. Ashanujjaman, S. Banik, G. Coloretti, A. Crivellin, S. P. Maharathy, and B. Mellado, “Explaining the $\gamma\gamma + X$ Excesses at ≈ 151.5 GeV via the Drell-Yan production of a Higgs triplet,” *Phys. Lett. B* **862** (2025) 139298, [arXiv:2402.00101 \[hep-ph\]](#).
 23. A. Crivellin, S. Ashanujjaman, S. Banik, G. Coloretti, S. P. Maharathy, and B. Mellado, “Growing evidence for a Higgs triplet*,” *Chin. Phys. C* **49** no. 5, (2025) 053107, [arXiv:2404.14492 \[hep-ph\]](#).
 24. S. Ashanujjaman, S. Banik, G. Coloretti, A. Crivellin, S. P. Maharathy, and B. Mellado, “Anatomy of the real Higgs triplet model,” *JHEP* **04** (2025) 003, [arXiv:2411.18618 \[hep-ph\]](#).
 25. S. P. Maharathy, P. Maroesh, P. Ndhlovu, S. Bhattacharya, A. Crivellin, M. Kumar, R. Mazini, and B. Mellado, “Discovery Prospects for the $Y = 0$ Scalar Triplet at Future e^+e^- Colliders,” [arXiv:2509.14378 \[hep-ph\]](#).
 26. ATLAS Collaboration, G. Aad et al., “Observation of VVZ production at $\sqrt{s} = 13$ TeV with the ATLAS detector,” *Phys. Lett. B* **866** (2025) 139527, [arXiv:2412.15123 \[hep-ex\]](#).
 27. CMS Collaboration, A. Hayrapetyan et al., “Measurement of WWZ and ZH Production Cross Sections at $s=13$ and 13.6 TeV,” *Phys. Rev. Lett.* **135** no. 9, (2025) 091802, [arXiv:2505.20483 \[hep-ex\]](#).
 28. J. Butterworth, H. Debnath, P. Fileviez Perez, and F. Mitchell, “Custodial symmetry breaking and Higgs boson signatures at the LHC,” *Phys. Rev. D* **109** no. 9, (2024) 095014, [arXiv:2309.10027 \[hep-ph\]](#).
 29. ATLAS Collaboration, G. Aad et al., “Observation of WWW Production in pp Collisions at $\sqrt{s}=13$ TeV with the ATLAS Detector,” *Phys. Rev. Lett.* **129** no. 6, (2022) 061803, [arXiv:2201.13045 \[hep-ex\]](#).
 30. CMS Collaboration, “Observation of tWZ production at the CMS experiment,”.
 31. CMS Collaboration, A. Hayrapetyan et al., “Measurements of inclusive and differential cross sections for top quark production in association with a Z boson in proton-proton collisions at $\sqrt{s} = 13$ TeV,” *JHEP* **02** (2025) 177, [arXiv:2410.23475 \[hep-ex\]](#).
 32. ATLAS Collaboration, G. Aad et al., “Inclusive and differential cross-section measurements of $t\bar{t}Z$ production in pp collisions at $\sqrt{s} = 13$ TeV with the ATLAS detector, including EFT and spin-correlation interpretations,” *JHEP* **07** (2024) 163, [arXiv:2312.04450 \[hep-ex\]](#).
 33. J. Alwall, R. Frederix, S. Frixione, V. Hirschi, F. Maltoni, O. Mattelaer, H. S. Shao, T. Stelzer, P. Torrielli, and M. Zaro, “The automated computation of tree-level and next-to-leading order differential cross sections, and their matching to parton shower simulations,” *JHEP* **07** (2014) 079, [arXiv:1405.0301 \[hep-ph\]](#).
 34. R. Frederix, S. Frixione, V. Hirschi, D. Pagani, H. S. Shao, and M. Zaro, “The automation of next-to-leading order electroweak calculations,” *JHEP* **07** (2018) 185, [arXiv:1804.10017 \[hep-ph\]](#). [Erratum: *JHEP* 11, 085 (2021)].
 35. T. Sjöstrand, S. Ask, J. R. Christiansen, R. Corke, N. Desai, P. Ilten, S. Mrenna, S. Prestel, C. O. Rasmussen, and P. Z. Skands, “An introduction to PYTHIA 8.2,” *Comput. Phys. Commun.* **191** (2015) 159–177, [arXiv:1410.3012 \[hep-ph\]](#).
 36. DELPHES 3 Collaboration, J. de Favereau, C. Delaere, P. Demin, A. Giammanco, V. Lemaitre, A. Mertens, and M. Selvaggi, “DELPHES 3, A modular framework for fast simulation of a generic collider experiment,” *JHEP* **02** (2014) 057, [arXiv:1307.6346 \[hep-ex\]](#).
 37. CMS Collaboration, A. M. Sirunyan et al., “Observation of the Production of Three Massive Gauge Bosons at $\sqrt{s}=13$ TeV,” *Phys. Rev. Lett.* **125** no. 15, (2020) 151802, [arXiv:2006.11191 \[hep-ex\]](#).
 38. C. G. Lester and D. J. Summers, “Measuring masses of semiinvisibly decaying particles pair produced at hadron colliders,” *Phys. Lett. B* **463** (1999) 99–103, [arXiv:hep-ph/9906349](#).
 39. A. Barr, C. Lester, and P. Stephens, “ $m(T_2)$: The Truth behind the glamour,” *J. Phys. G* **29** (2003) 2343–2363, [arXiv:hep-ph/0304226](#).
 40. LHC Higgs Cross Section Working Group Collaboration, J. R. Andersen et al., “Handbook of LHC

- Higgs Cross Sections: 3. Higgs Properties,”
[arXiv:1307.1347](#) [[hep-ph](#)].
41. S. Ashanujjaman, A. Crivellin, S. P. Maharathy, and B. Mellado, “Searching for a Charged Higgs Boson in Top-Quark Decays via the WZ Mode,”
[arXiv:2509.07094](#) [[hep-ph](#)].
 42. P. H. Chankowski, S. Pokorski, and J. Wagner, “(Non)decoupling of the Higgs triplet effects,” *Eur. Phys. J. C* **50** (2007) 919–933, [arXiv:hep-ph/0605302](#).
 43. T. Blank and W. Hollik, “Precision observables in $SU(2) \times U(1)$ models with an additional Higgs triplet,” *Nucl. Phys. B* **514** (1998) 113–134, [arXiv:hep-ph/9703392](#).
 44. J. R. Forshaw, A. Sabio Vera, and B. E. White, “Mass bounds in a model with a triplet Higgs,” *JHEP* **06** (2003) 059, [arXiv:hep-ph/0302256](#).
 45. M.-C. Chen, S. Dawson, and T. Krupovnickas, “Higgs triplets and limits from precision measurements,” *Phys. Rev. D* **74** (2006) 035001, [arXiv:hep-ph/0604102](#).
 46. R. S. Chivukula, N. D. Christensen, and E. H. Simmons, “Low-energy effective theory, unitarity, and non-decoupling behavior in a model with heavy Higgs-triplet fields,” *Phys. Rev. D* **77** (2008) 035001, [arXiv:0712.0546](#) [[hep-ph](#)].
 47. P. Bandyopadhyay and A. Costantini, “Obscure Higgs boson at Colliders,” *Phys. Rev. D* **103** no. 1, (2021) 015025, [arXiv:2010.02597](#) [[hep-ph](#)].
 48. P. Fileviez Perez, H. H. Patel, M. J. Ramsey-Musolf, and K. Wang, “Triplet Scalars and Dark Matter at the LHC,” *Phys. Rev. D* **79** (2009) 055024, [arXiv:0811.3957](#) [[hep-ph](#)].